

Spin Squeezing Property of Weighted Graph States

Peng Xue

Department of Physics, Southeast University, Nanjing 211189, China

(Dated: December 2, 2024)

We study the spin squeezing property of weighted graph states, which can be used to improve the sensitivity in interferometry. Decoherence reduces the spin squeezing property but the result remains superior over other reference schemes with GHZ-type maximally entangled states and product states. We study the time evolution of spin squeezing of weighted graph states coupled to different decoherence channels. Based on the analysis, the spin squeezing of the weighted graph states is robust in the presence of decoherence and the decoherence limit in the improvement of the interferometric sensitivity is still achievable.

PACS numbers: 06.30.Ft, 03.65.Yz, 03.67.Pp, 06.20.Dk

I. INTRODUCTION

Quantum correlations have attracted much interest as intriguing manifestation of nonclassical phenomena and they have also found many promising applications such as achieving interferometric [1–4] and spectroscopic [5] sensitivities beyond the standard quantum noise limit using squeezed states and GHZ-type maximally entangled states. The spin squeezed states are quantum correlated states [6] with reduced fluctuations in one of the collective spin components, with possible applications in atomic interferometers and high-precision atomic clocks. Entanglement is based on the superposition principle combined with the Hilbert space structure, while squeezing is originated from another fundamental principle of quantum mechanics—the uncertainty principle. Therefore, it is interesting and important to study their relationship and different applications. It is found that spin squeezing and entanglement are closely related and spin squeezing implies entanglement [7, 8]. In this paper we will study their different robustness to the quantum noise and decoherence.

To evaluate the potential application of quantum correlations such as spin squeezing and entanglement, it is therefore essential to include a realistic description of noise in experiments of interests. In this paper, we analyze the effect of realistic decoherence processes and noise sources shot-noise phase sensitivity $\delta\varphi$ in estimation of a collective rotation angle φ .

In the absence of decoherence, the squeezed uncertainty of a transverse spin component directly improves the sensitivity in interferometry [3], enabling the improvement factors up to $N^{1/3}$ for one-axis twisting and $N^{1/2}$ for two-axis twisting with N particles [9]. GHZ-type maximally entangled states can also improve interferometric sensitivity by a factor of $N^{1/2}$ treating N particles as a single quantum object. The phase evolution of an object consisting of N particles is N times as fast as that of a particle itself, or an equivalently deBroglie wavelength is shortened by a factor of N , giving the standard quantum limit for an object ~ 1 [10].

In the presence of decoherence, a GHZ type maximally entangled state with zero spin squeezing parameter does not provide higher resolution compared to product states [4, 11–13]. Whereas a partially entangled state with a high symmetry such as a weighted graph state gives an improved sensitivity. Thus in the presence of decoherence the spin squeezing results the improvement the sensitivity in interferometry. To find weighted graph states whose spin squeezing property is robust to decoherence [14, 15] is the aim of this paper. Graph states proved very robust against many sources of noise [16–18]. In this paper we will study a special kind of graph states—weighted graph states and combine the robustness of the spin squeezing property of these states with a scheme capable of improving interferometric sensitivity.

A weighted graph state is a multipartite entangled state consisting of a set of vertices j connected to each other by edges taking the form of controlled phase gate [19, 20]. The qubits are prepared in $|+\rangle_j$, where $|\pm\rangle_j = (|\downarrow\rangle \pm |\uparrow\rangle)_j / \sqrt{2}$ and $\{|\downarrow\rangle_j, |\uparrow\rangle_j\}$ is the single-qubit computational basis. The weights $\alpha_{jk} \in [0, 2\pi]$ correspond to a controlled phase operation applied between the two vertices j and k . Weighted graph states are a $O(N^2)$ parameter family of N -spin state, correspond to weighted graphs which are independent of the geometry and adaptable to arbitrary geometries and spatial dimensions [21].

This paper is organized as follows. Firstly we introduce the definitions of spin squeezing parameters in Sec. II. In Sec. III, the generation of weighted graph states and the spin squeezing property of weighted graph states are introduced. The evolution of the spin squeezing of the weighted graph states coupled to three kinds of decoherence channels is shown in Sec. IV and then we analyze the robustness of the spin squeezing of weighted graph states against decoherence. In Sec. V, we discuss the application of the spin squeezing property of weighted graph states—to improve the frequency standard in the presence of decoherence. Finally we briefly summarize the paper in Sec. VI.

II. SPIN SQUEEZING DEFINITIONS

The definition of spin-squeezing is not unique, and in the section we review two most widely studied squeezing parameters proposed by Kitagawa and Ueda [3] and by Wineland et al. [5].

We consider an ensemble of N two-level particles with lower (upper) state $|\downarrow\rangle$ ($|\uparrow\rangle$). Adopting the nomenclature of spin-1/2 particles, we introduce the total angular momentum (i.e., Bloch vector)

$$\vec{J} = \sum_{j=1}^N \vec{S}_j, \quad (1)$$

where

$$\vec{S}_z^j = \frac{1}{2} \hat{\sigma}_z^j = \frac{1}{2} \left(|\uparrow\rangle_j \langle\uparrow| - |\downarrow\rangle_j \langle\downarrow| \right). \quad (2)$$

At this point, it is convenient to introduce the following two kinds of spin squeezing parameters [5, 22]

$$\begin{aligned} \xi_1^2 &= \frac{4(\Delta J_{\vec{n}_\perp})_{\min}^2}{N}, \\ \xi_2^2 &= \frac{N^2}{4\langle\vec{J}\rangle^2} \xi_1^2. \end{aligned} \quad (3)$$

Here, the minimization in the first equation is over all directions denoted by \vec{n}_\perp , perpendicular to the mean spin direction $\vec{n} = \langle\vec{J}\rangle/|\langle\vec{J}\rangle|$. If $\xi_2^2 < 1$ is satisfied, the spin squeezing occurs and the N -qubit state is entangled.

It is known that the spin squeezing manifested by $\xi_2^2 < 1$ leads to improvement in the frequency measurement [4, 11]. Generally speaking, an interferometer is quantum mechanically described as a collective, linear, rotation of input state by an angle φ :

$$\rho_{\text{out}}(\varphi) = e^{i\varphi\vec{J}_{\vec{n}}} \rho_{\text{in}} e^{-i\varphi\vec{J}_{\vec{n}}}. \quad (4)$$

The goal is to estimate φ with a sensitivity overcoming the standard quantum limit or shot-noise limit $\delta\varphi = 1/\sqrt{N}$ [13].

Spin squeezed states are multiqubit entangled states showing pairwise entanglement and reduced uncertainty in the collective spin moment in one direction. This reduction in the measurement uncertainty, achieved without violating the minimum uncertainty principle by a redistribution of the quantum fluctuations between noncommuting variables can be exploited to perform metrology beyond the Heisenberg limit. The degree of squeezing of a spin ensemble is evaluated by the squeezing parameter ξ_2^2 . When spin squeezing is instead used in the context of quantum limited metrology, the squeezing parameter should measure the improvement in signal-to-noise ratio for the measured quantity φ and the phase sensitivity is

$$\delta\varphi = \frac{\xi_2}{\sqrt{N}}. \quad (5)$$

This definition is associated to Ramsey-type experiments [23], in which an external magnetic field is measured via the detection of the accumulated phase φ due to the Zeeman interaction and the phase uncertainty for a product state is $\sim \sqrt{N}$, and for a GHZ-type maximally entangled state is $\sim N$ in the absence of decoherence. If $\xi_2 < 1$, $\delta\varphi$ beats the shot-noise limit. In the limit of large spin numbers, using the one- and two-axis squeezing operator, the optimal squeezing parameters are $\xi_1^2 \sim 3^{2/3}/(2N^{2/3})$ [9] and $\xi_2^2 \sim (1 + 2\sqrt{3})/(2N)$ [24, 25], respectively.

III. SPIN SQUEEZING PROPERTY OF WEIGHTED GRAPH STATES

We introduce so-called weighted graph states in the section. We begin by defining a graph, $G = (V, E)$, as a finite non-empty point set V with a collective $E \subset V$ of unordered pairs of points in V . And V is the collection of edges. Graphs such as these can be used to describe a family of quantum states in the following manner. The initial states are prepared in $|+\rangle^{\otimes N}$. Between each pair of qubits connected by an edge in the associated graph, we apply a unitary operation—controlled phase operation. Weighted graph states naturally arise when spin system interact via an Ising-type interaction.

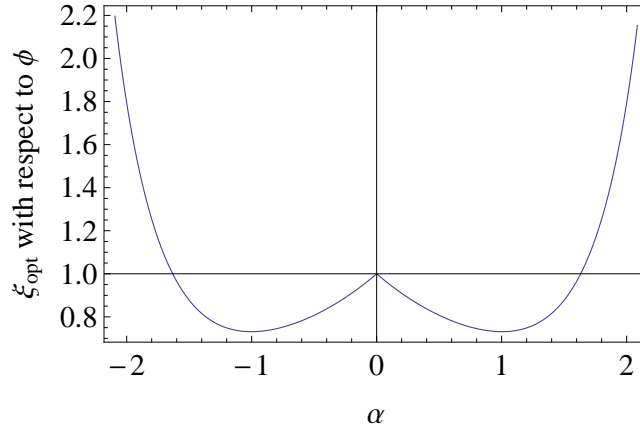


FIG. 1: Simulation of spin squeezing parameter for weighted cluster state ξ_2 minimized with respect to ϕ as a function of α .

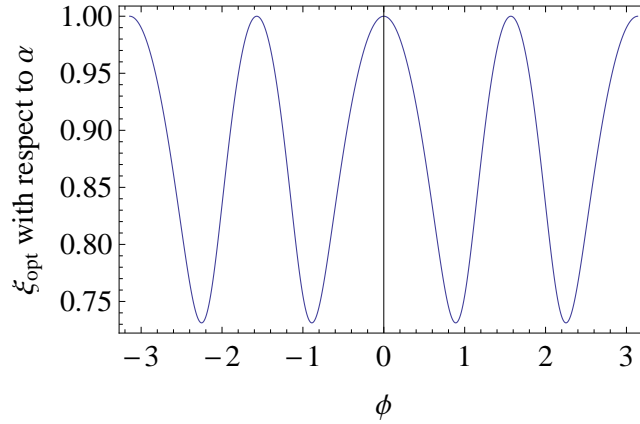


FIG. 2: Simulation of spin squeezing parameter for weighted cluster state ξ_2 minimized with respect to α as a function of ϕ .

We consider N spin-1/2 system with pairwise interactions described by an Ising-type Hamiltonian

$$\hat{H} = \sum_{j,k} \frac{1}{4} f(j,k) (\mathbb{I} - \hat{\sigma}_z^j) \otimes (\mathbb{I} - \hat{\sigma}_z^k). \quad (6)$$

The weighted graph state [16, 17] is obtained by the evolution of the above Hamiltonian

$$|\psi_t\rangle = \exp(-i\hat{H}t) |+\rangle^{\otimes N} \propto \prod_{j,k} \exp\left[-\frac{1}{4} i f(j,k) t \hat{\sigma}_z^j \hat{\sigma}_z^k\right] |+\rangle^{\otimes N}. \quad (7)$$

If we choose the evolution time to satisfy $f(j,k)t = m\pi$ with m an integer, the state $|\psi_t\rangle$ is a product state. If $f(j,k)t = (2m+1)\pi/2$, $|\psi_t\rangle$ becomes a graph state. And for $0 < f(j,k)t < \pi/2$, $|\psi_t\rangle$ is a weighted graph state with spin squeezing parameter $\xi_2 < 1$.

In this paper we only consider two kinds of simplest weighted graph states—weighted cluster states and weighted fully-connected graph states. For the weighted cluster state we have the form

$$|\psi_t\rangle = \prod_{j=1}^{N-1} \exp\left[-\frac{i}{4} f_j t (\mathbb{I} - \hat{\sigma}_z^j) \otimes (\mathbb{I} - \hat{\sigma}_z^{j+1})\right] |+\rangle^{\otimes N}. \quad (8)$$

If we make our case further simpler by assuming $f_j \equiv f$ for each qubit j of the weighted cluster state and $ft \equiv \alpha$, the spin squeezing parameter takes this form

$$\xi_2^2 = \frac{1 + \cos^2 \phi \sin^2 \alpha/2 + \sin 2\phi \sin \alpha}{\cos^4 \alpha/2} \quad (9)$$

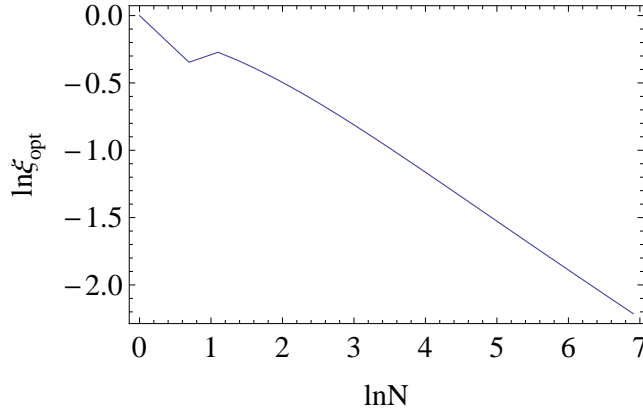


FIG. 3: Ln-ln plot of the spin squeezing parameter for weighted fully- connected graph state ξ_2 v.s. the number of the qubits N (up to 10^3) optimized with respect to α .

with the mean spin direction

$$\vec{n} = (\cos \alpha, \sin(-\alpha), 0), \quad (10)$$

the orthogonal direction

$$\vec{n}_\perp = (-\cos \phi \sin(-\alpha), \cos \phi \cos \alpha, \sin \phi), \quad (11)$$

and $\phi \in [-\pi, \pi]$. The spin squeezing parameter is independent of the number of the qubits N and can be optimized to be $\xi_{\min} = 0.7312$ with respect to α and ϕ shown in Figs. 1 and 2.

For the weighted fully-connected graph state, we have the form

$$|\psi_t\rangle = \prod_{j \neq k} \exp \left[-\frac{i}{4} \alpha (\mathbb{I} - \hat{\sigma}_z^j) \otimes (\mathbb{I} - \hat{\sigma}_z^k) \right] |+\rangle^{\otimes N}. \quad (12)$$

The spin squeezing parameter of the weighted fully-connected graph state with the same weight α takes this form

$$\xi_2^2 = \frac{1 - (N-1) [\sqrt{A^2 + B^2} - A] / 4}{\cos^{2N-2} \alpha}, \quad (13)$$

where

$$A = 1 - \cos^{N-2}(2\alpha), B = 4 \sin \alpha \cos^{N-2} \alpha. \quad (14)$$

The mean spin direction for the weighted fully-connected graph state is

$$\vec{n} = (\cos(N\alpha), \sin(-N\alpha), 0), \quad (15)$$

and the orthogonal direction is then

$$\vec{n}_\perp = (-\cos \phi \sin(-N\alpha), \cos \phi \cos(N\alpha), \sin \phi). \quad (16)$$

The minimum spin squeezing parameter with respect to α is obtained $\xi_2 \propto 1/N^{1/3}$ shown in Fig. 3.

IV. EVOLUTION OF SPIN SQUEEZING OF WEIGHTED GRAPH STATES IN THE PRESENCE OF DECOHERENCE

The decoherence effects are described by three types of decoherence channels: the amplitude damping channel, the dephasing channel, and the depolarizing channel. In general, decoherence process can be described by these three typical channels.

We consider a single qubit coupled to an environment which is described by a thermal reservoir. The evolution of this qubit is governed by a general master equation of Lindblad form

$$\frac{\partial \chi}{\partial t} = -i [\hat{H}_r, \chi] + \mathcal{L}\chi, \quad (17)$$

where the reference system is the standard system used in phase sensitivity and it is defined as

$$\hat{H}_r = \frac{\Delta}{2} \sum_{j=1}^N \hat{\sigma}_z^j. \quad (18)$$

Whereas, the incoherent processes are described by the superoperator \mathcal{L} :

$$\begin{aligned} \mathcal{L}\chi = & -\frac{b}{2}(1-s) [\hat{\sigma}_+ \hat{\sigma}_- \chi + \chi \hat{\sigma}_+ \hat{\sigma}_- - 2\hat{\sigma}_- \chi \hat{\sigma}_+] - \frac{b}{2}s [\hat{\sigma}_- \hat{\sigma}_+ \chi + \chi \hat{\sigma}_- \hat{\sigma}_+ - 2\hat{\sigma}_+ \chi \hat{\sigma}_-] \\ & - \frac{2c-b}{8} [2\chi - 2\hat{\sigma}_z \chi \hat{\sigma}_z], \end{aligned} \quad (19)$$

with $\hat{\sigma}_\pm = (\hat{\sigma}_x \pm i\hat{\sigma}_y)/2$. For an arbitrary s , $b = 0$ and $c = \gamma$, the qubit is coupled to a dephasing channel. For $s = 1/2$ and $b = c = \gamma$, the qubit is coupled to a depolarizing channel. Whereas, for $s = 1$ and $b = 2c = \gamma$, that is coupled to a decay channel (pure damping).

Equivalently, one can use the resulting completely positive map \mathcal{E} with $\chi' = \mathcal{E}\chi$ as follows:

$$\mathcal{E}\chi = \sum_{j=0}^3 p_j(t) \hat{\sigma}_j \chi \hat{\sigma}_j. \quad (20)$$

with χ a density matrix for a single-qubit state and $\sum_{j=0}^3 p_j(t) = 1$. These noise channels are of particles interest in quantum information theory, especially in the study of fault-tolerance of quantum computation. This class contains for example: (i) for $p_0 = (1 + 3e^{-\gamma t})/4$ and $p_1 = p_2 = p_3 = (1 - e^{-\gamma t})/4$ the above depolarizing channel; (ii) for $p_0 = (1 + e^{-\gamma t})/2$, $p_1 = p_2 = 0$ and $p_3 = (1 - e^{-\gamma t})/2$ the above dephasing channel. Finally, the decay channel is obtained:

$$\mathcal{E}\chi = E_0 \chi E_0^\dagger + E_1 \chi E_1^\dagger, \quad (21)$$

with the Kraus operators $E_0 = \begin{pmatrix} 1 & 0 \\ 0 & e^{-\gamma t/2} \end{pmatrix}$ and $E_1 = \begin{pmatrix} 0 & \sqrt{1 - e^{-\gamma t}} \\ 0 & 0 \end{pmatrix}$ [17].

For a system consisting of N two-level particles, we would be interested in the effect of decoherence on the spin squeezing properties of this system. We consider as a decoherence model individual coupling of each of the qubits to a thermal bath, where the evolution of the k th qubit is described by the map \mathcal{E}_k with Pauli operators $\hat{\sigma}_j$ ($j = 0, 1, 2, 3$) acting on qubit k . We would be interested in the evolution of a given weighted graph state ψ of N qubit under this decoherence model. That is, the initial state ψ suffers from decoherence and evolves in time to a mixed state $\rho(t)$ given by

$$\rho(t) = \mathcal{E}_1 \mathcal{E}_2 \dots \mathcal{E}_N |\psi_t\rangle \langle \psi_t|. \quad (22)$$

Entangled states are known to decay more rapidly due to decoherence than product states. So that in practice the improvement in sensitivity is often counterbalanced by the need to reduce the interrogation time. In particular, if the system is prepared in the GHZ-type maximally entangled state the sensitivity improvement is completely lost in the presence of some classes of decoherence such as dephasing, as the system is N -time more sensitivity both to the signal and the noise. A partially entangled state with spin squeezing robust to decoherence, such as a weighted graph state, can instead provide an advantage over product states or GHZ-type maximally entangled states.

For the weighted cluster state, we can easily evaluate the modified main spin direction in the presence of dephasing as

$$\vec{n}' = (\cos(\Delta t - \alpha), \sin(\Delta t - \alpha), 0), \quad (23)$$

and the modified orthogonal direction is

$$\vec{n}'_\perp = (-\cos\phi \sin(\Delta t - \alpha), \cos\phi \cos(\Delta t - \alpha), \sin\phi). \quad (24)$$

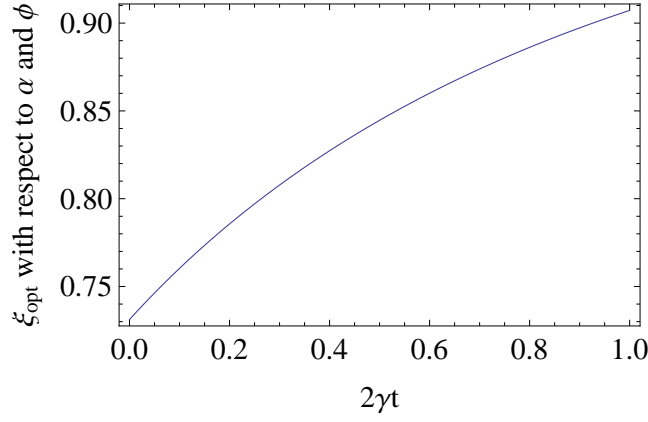


FIG. 4: In the individual dephasing channel, the spin squeezing parameter of the weighted cluster state ξ_2 as a function of $2\gamma t$ optimized with respect to α and ϕ .

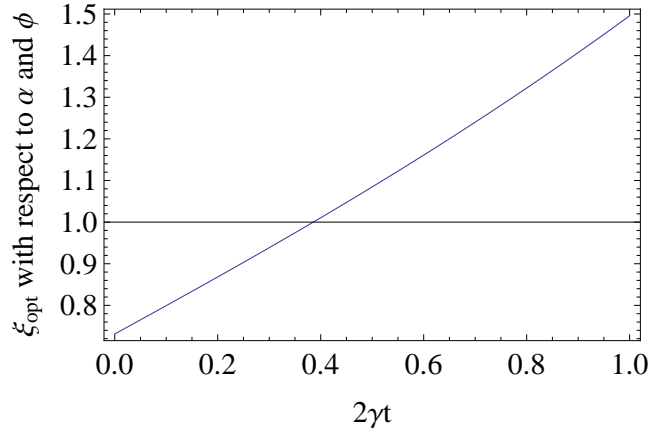


FIG. 5: In the individual depolarizing channel, the spin squeezing parameter of the weighted cluster state ξ_2 as a function of $2\gamma t$ optimized with respect to α and ϕ .

Then the spin squeezing parameter of the weighted cluster state evolves to

$$\xi_2^2(t) = \frac{1 + e^{-2\gamma t} \cos^2 \phi \sin^2 \alpha/2 + e^{-\gamma t} \sin 2\phi \sin \alpha}{\cos^4 \alpha/2}. \quad (25)$$

in the individual dephasing channel, which is the main type of decoherence for a spin ensemble. Coupling to the individual depolarizing channel, the spin squeezing parameter of the weighted cluster state evolves to

$$\xi_2^2(t) = \frac{1 + e^{-2\gamma t} \cos^2 \phi \sin^2 \alpha/2 + e^{-\gamma t} \sin 2\phi \sin \alpha}{e^{-2\gamma t} \cos^4 \alpha/2}. \quad (26)$$

Whereas, the spin squeezing parameter of the weighted cluster state evolves to

$$\xi_2^2(t) = \frac{1 + e^{-\gamma t} \cos^2 \phi \sin^2 \alpha/2 + e^{-\gamma t} \sin 2\phi \sin \alpha}{\left[1 + e^{-\gamma t} (\cos^2 \alpha/2 - 1)^2\right]^2} \quad (27)$$

in the individual damping channel.

Figs. 4-6 show the dynamics of the spin squeezing parameter of the weighted cluster states coupled to different noisy channels. For three different noisy channels, the optimized spin squeezing parameter increases with time. In Figs. 4 and 6, coupled to the individual dephasing and damping channel the spin squeezing property of the weighted cluster state still holds (< 1) for $0 < 2\gamma t < 1$. In Fig. 5, in the individual depolarizing channel, the spin squeezing parameter of the weighted cluster state is smaller than 1 for small damping parameter $2\gamma t < 0.398$.

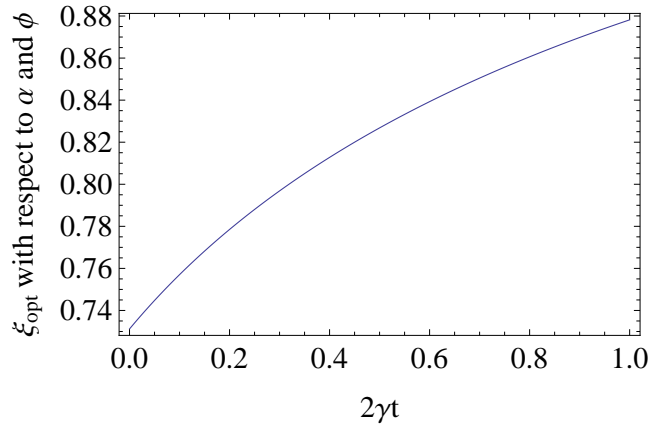


FIG. 6: In the individual pure damping channel, the spin squeezing parameter of the weighted cluster state ξ_2 as a function of $2\gamma t$ optimized with respect to α and ϕ .

$2\gamma t$	ζ	$\Delta\zeta$	δ
0	-0.3372	0.009	0.2730
0.25	-0.2643	0.013	0.0298
0.5	-0.1813	0.014	-0.1173
0.75	-0.1348	0.022	-0.1455
1	-0.1064	0.030	-0.1338

TABLE I: The linear regression data $\ln\xi_2 = (\zeta \pm \Delta\zeta)\ln N + \delta$ of the dynamics of the spin squeezing of weighted fully-connected graph state in the individual dephasing channel with different dephasing parameters.

For the weighted fully-connected graph state, we consider the same dephasing channel. The modified mean spin direction and the orthogonal direction are calculated as

$$\begin{aligned}\vec{n}' &= (\cos(\Delta t - N\alpha), \sin(\Delta t - N\alpha), 0), \\ \vec{n}'_{\perp} &= (-\cos\phi \sin(\Delta t - N\alpha), \cos\phi \cos(\Delta t - N\alpha), \sin\phi).\end{aligned}\quad (28)$$

Coupling to the individual dephasing channel which is the main type of decoherence for a spin ensemble, the spin squeezing parameter of the weighted fully-connected graph state evolves to

$$\xi_2^2(t) = \frac{1 + \frac{1}{4}e^{-2\gamma t}(N-1)\left(A - \frac{A^2}{\sqrt{A^2+B^2}}\right) - \frac{1}{4}e^{-\gamma t}(N-1)\frac{B^2}{\sqrt{A^2+B^2}}}{\cos^{2N-2}\alpha}.\quad (29)$$

Then the spin squeezing parameter of the weighted fully-connected state evolves to

$$\xi_2^2(t) = \frac{1 + \frac{1}{4}e^{-2\gamma t}(N-1)\left(A - \frac{A^2}{\sqrt{A^2+B^2}}\right) - \frac{1}{4}e^{-\gamma t}(N-1)\frac{B^2}{\sqrt{A^2+B^2}}}{e^{-2\gamma t}\cos^{2N-2}\alpha}.\quad (30)$$

under the individual depolarizing. Whereas, the spin squeezing parameter of the weighted fully-connected graph state evolves to

$$\xi_2^2(t) = \frac{1 + \frac{1}{4}e^{-\gamma t}(N-1)\left(A - \frac{A^2}{\sqrt{A^2+B^2}}\right) - \frac{1}{4}e^{-\gamma t}(N-1)\frac{B^2}{\sqrt{A^2+B^2}}}{[e^{-\gamma t}\cos^{N-1}\alpha - (1 - e^{-\gamma t})]^2}.\quad (31)$$

in the individual damping channel.

Figs. 7-9 show $\ln\text{-}\ln$ plots of the spin squeezing parameter ξ_2 of the weighted fully-connected graph state coupled to different noisy channels including dephasing, depolarizing and damping channels v.s. the number of qubits N optimized with respect to α . In Figs. 7 and 8 the simulated results on the spin squeezing parameter of the weighted fully-connected graph state coupled to the individual dephasing and depolarizing channels respectively are shown and both follow a power law on the particle number N , thus $\ln\xi_2 = \zeta\ln N + \delta$. Corresponding linear regression data presented in Tables I and II clearly reveals slopes decrease with the decoherence rates increasing. Fig. 9 shows the spin squeezing of weighted fully-connected graph state coupled to individual damping channel, which is not linear any more but for large N the spin squeezing property still holds.

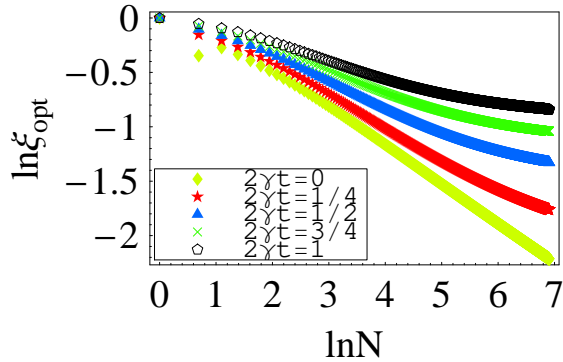


FIG. 7: Ln-ln plots of the spin squeezing parameters ξ_2 of the weighted fully-connected graph state v.s. the number of the qubits N (up to 10^3) with different dephasing rate γ : $2\gamma t = 0$ (yellow diamonds), $2\gamma t = 0.25$ (red stars), $2\gamma t = 0.5$ (blue triangles), $2\gamma t = 0.75$ (green crosses), $2\gamma t = 1$ (black circles).

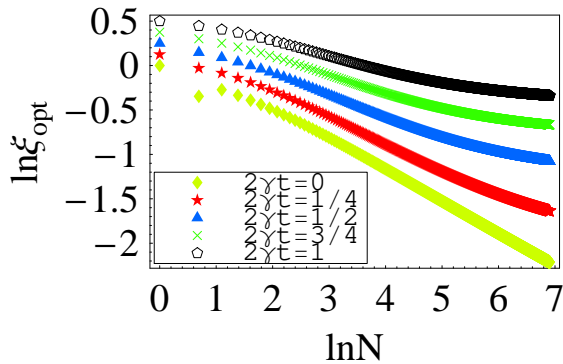


FIG. 8: Ln-ln plots of the spin squeezing parameters ξ_2 of the weighted fully-connected graph state v.s. the number of the qubits N (up to 10^3) with different depolarizing rate γ : $2\gamma t = 0$ (yellow diamonds), $2\gamma t = 0.25$ (red stars), $2\gamma t = 0.5$ (blue triangles), $2\gamma t = 0.75$ (green crosses), $2\gamma t = 1$ (black circles).

V. APPLICATIONS

As we mentioned in Sec. II, the spin squeezing can be used to improve the frequency standards. In the absence of decoherence, using the product state with N qubits the phase sensitivity is $\delta\varphi \propto 1/\sqrt{N}$ and using the N -qubit maximally entangled state such as GHZ state the phase sensitivity can be improved to be $\delta\varphi \propto 1/N$. Hence, the squeezed uncertainty of a transverse spin component directly improves the sensitivity in interferometry including Ramsey spectroscopy, enabling the improvement factors up to \sqrt{N} for GHZ states with N particles. In the presence of decoherence, one will obtain the same accuracy for frequency standards for GHZ states as [11]

$$\delta\varphi_{\text{GHZ}} = \frac{\sqrt{2\gamma t e}}{\sqrt{N}} \propto \frac{1}{\sqrt{N}}. \quad (32)$$

That means there is no improvement even with GHZ-type maximally entangled states. However with one of partial entangled states—weighted fully-connected graph states the sensitivity is still reduced in the presence of decoherence but our scheme remains superior over several reference schemes with states such as GHZ-type states and product states because of the robustness of spin squeezing property.

In linear interferometry, the phase precision for an N -particle weighted fully-connected graph state can be explained by classical statistics. The situation is equivalent to N individual measurements on a single particle [26]. The minimal phase error for a classical measurement $\delta\varphi = 1/\sqrt{N}$ is known as the standard quantum limit. In the case of correlated particles, the classical limit can be exceeded. The idea is to achieve improved scaling of the interferometric phase sensitivity with the number of particles using entangled states within the interferometer [13, 27] as low as the Heisenberg limit, where the phase error is $\delta\varphi = 1/N$. A weighted fully-connected graph state is a special kind of

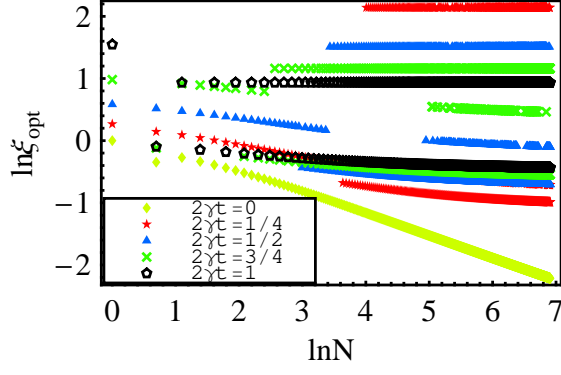


FIG. 9: Ln-ln plots of the spin squeezing parameters ξ_2 of the weighted fully-connected graph state v.s. the number of the qubits N (up to 10^3) with different damping rate γ : $2\gamma t = 0$ (yellow diamonds), $2\gamma t = 0.25$ (red stars), $2\gamma t = 0.5$ (blue triangles), $2\gamma t = 0.75$ (green crosses), $2\gamma t = 1$ (black circles).

$2\gamma t$	ζ	$\Delta\zeta$	δ
0	-0.3372	0.006	0.2730
0.25	-0.2643	0.009	0.1548
0.5	-0.1813	0.013	0.1327
0.75	-0.1348	0.030	0.2295
1	-0.1064	0.034	0.3662

TABLE II: The linear regression data $\ln\xi_2 = (\zeta \pm \Delta\zeta)\ln N + \delta$ of the dynamics of the spin squeezing of weighted fully-connected graph state in the individual depolarizing channel with different depolarizing parameters.

many-particle spin squeezing state for which the minimal interferometric phase error is

$$\delta\varphi = \frac{\xi_2}{\sqrt{N}}. \quad (33)$$

If the relation between the phase error $\delta\phi$ with the particle number is a power law, then we define

$$\ln\delta\varphi = -\varsigma\ln N + \ln\delta\varphi_0, \quad (34)$$

with $\varsigma = 1$ for the Heisenberg limit, $\varsigma = 1/2$ for the classical limit and $1/2 < \varsigma < 1$ means that the weighted fully-connected graph state can still be used to improve the frequency standard.

In the presence of decoherence, Huelge *et al.* [11] have shown that a GHZ-type maximally entangled state does not provide an improved sensitivity compared to product states. We show here that a weighted fully-connected graph state

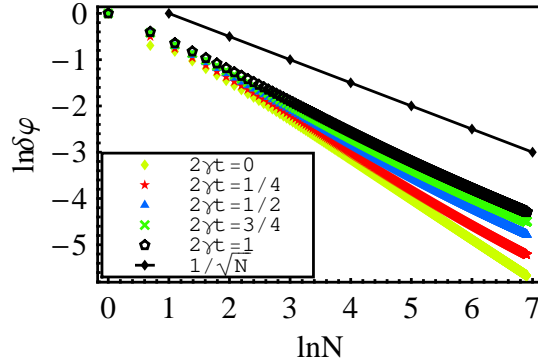


FIG. 10: Ln-ln plots of the phase error $\delta\varphi$ v.s. the number of the qubits N (up to 10^3) with different dephasing rate γ : $2\gamma t = 0$ (yellow diamonds), $2\gamma t = 0.25$ (red stars), $2\gamma t = 0.5$ (blue triangles), $2\gamma t = 0.75$ (green crosses), $2\gamma t = 1$ (black circles). The solid black line presents the shot-noise limit $\delta\varphi \propto 1/\sqrt{N}$.

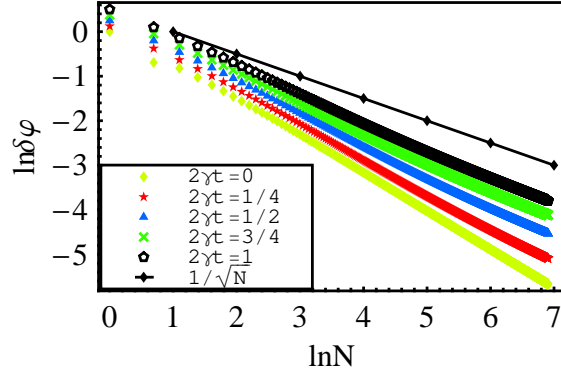


FIG. 11: Ln-ln plots of the phase error $\delta\varphi$ v.s. the number of the qubits N (up to 10^3) with different depolarizing rate γ : $2\gamma t = 0$ (yellow diamonds), $2\gamma t = 0.25$ (red stars), $2\gamma t = 0.5$ (blue triangles), $2\gamma t = 0.75$ (green crosses), $2\gamma t = 1$ (black circles). The solid black line presents the shot-noise limit $\delta\varphi \propto 1/\sqrt{N}$.

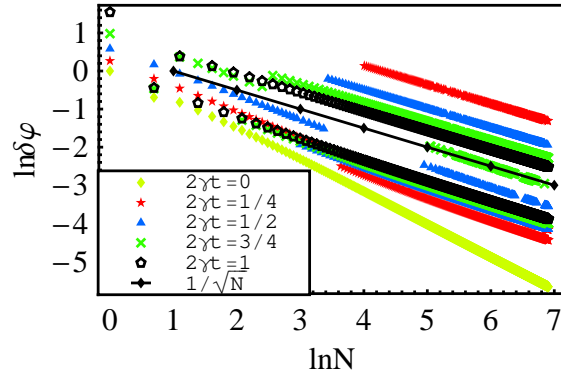


FIG. 12: Ln-ln plots of the phase error $\delta\varphi$ v.s. the number of the qubits N (up to 10^3) with different damping rate γ : $2\gamma t = 0$ (yellow diamonds), $2\gamma t = 0.25$ (red stars), $2\gamma t = 0.5$ (blue triangles), $2\gamma t = 0.75$ (green crosses), $2\gamma t = 1$ (black circles). The solid black line presents the shot-noise limit $\delta\varphi \propto 1/\sqrt{N}$.

with a high symmetry gives an improved sensitivity under the three kinds of decoherence—dephasing, depolarizing and damping.

For example, by optimizing with respect to the weights α , the spin squeezing parameter of the weighted fully-connected graph state is obtained numerically $\xi_2 \propto 1/N^{0.1064}$ with the decoherence rate (dephasing or depolarizing) satisfying $2\gamma t = 1$ shown in Figs. 7 and 8. Thus the phase sensitivity $\delta\varphi \propto 1/N^{0.6064}$ follows a power law on the number of the particles not a constant in Figs. 10 and 11. In Fig. 12 just as the spin squeezing parameter, ln-ln plot of the phase sensitivity under the damping v.s. the particle number is not linear any more. However from the slopes of the plot we can see find for some N the spin squeezing holds and the sensitivity can still be improved with the weighted fully-connected graph state coupled to individual damping channels.

We compare the schemes on improve the phase sensitivity with weighted fully-connected graph states and product states and prove that with weighted fully-connected graph states an improvement in the phase sensitivity is achieved beyond shot-noise limit. Now we compare our scheme to that with GHZ-type entangled states with same decoherent rate and evolution time. We define an improvement in the sensitivity

$$P = \frac{\delta\varphi_{\text{GHZ}}}{\delta\varphi} = \frac{\sqrt{2\gamma t e}}{\xi_2}. \quad (35)$$

If $P > 1$ the phase error in the scheme with a weighted fully-connected graph states is smaller than that with a GHZ state with same decoherent rate and evolution time and we have an improvement in the sensitivity. Remarkably, Figs. 13-15 show that for small N , $P < 1$ that means the phase error in the scheme with GHZ states is smaller than that with weighted full-connected graph states. However with N increasing our scheme shows its advantage. From numerical calculations with N up to 10^3 , we have an improvement $P \sim 4.5$ under dephasing and $P \sim 3.5$ under

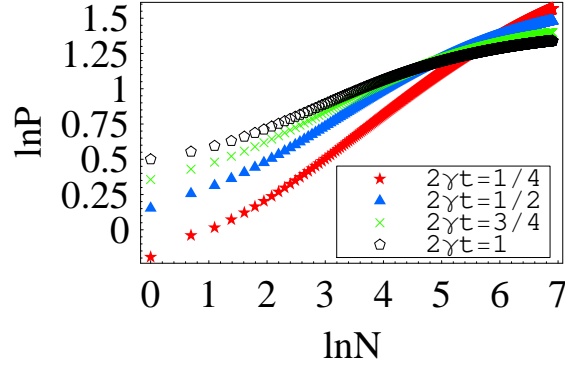


FIG. 13: Ln-ln plots of the improvement in the sensitivity P v.s. the number of the qubits N (up to 10^3) with different dephasing rate γ : $2\gamma t = 0$ (yellow diamonds), $2\gamma t = 0.25$ (red stars), $2\gamma t = 0.5$ (blue triangles), $2\gamma t = 0.75$ (green crosses), $2\gamma t = 1$ (black circles).

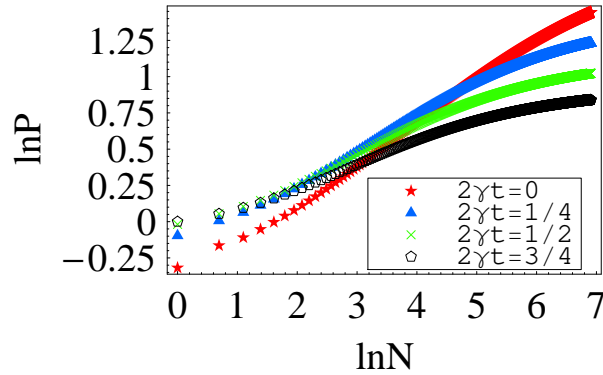


FIG. 14: Ln-ln plots of the improvement in the sensitivity P v.s. the number of the qubits N (up to 10^3) with different depolarizing rate γ : $2\gamma t = 0$ (yellow diamonds), $2\gamma t = 0.25$ (red stars), $2\gamma t = 0.5$ (blue triangles), $2\gamma t = 0.75$ (green crosses), $2\gamma t = 1$ (black circles).

depolarizing with respect to the shot noise limit $\sim 1/N^{0.5}$.

VI. CONCLUSION

The Heisenberg scaling $1/N$ in the decoherence-free case can be achieved. In the absence of decoherence, both of the weighted graph states and maximally entangled states are used to improve interferometric sensitivity. Whereas, in the presence of decoherence the ability of improving sensitivity is due to the robustness against decoherence. The open question is if the decoherence limit in the improvement without any measurement optimization is achieved with all the known weighted graph states. Our goal is to prove that it is spin squeezing instead of entanglement which improves the sensitivity and find out the weighted graph states whose spin squeezing property is robust to decoherence. Based on the analysis, in the presence of decoherence, when N is large enough, the phase sensitivity can not be improved any more via the maximally entangled states and product states, while the scheme with weighted graph states still survive and $\delta\varphi$ beats the shot-noise limit without any measurement optimization. Furthermore, one can obtain the optimal improvement of sensitivity by tuning the weighted of each edges and choosing proper joint measurements.

Acknowledgments

This work was performed during a sabbatical year at Key Lab of Quantum Information, Chinese Academy of Sciences. The author thanks Yongsheng Zhang and Xiangfa Zhou for useful conversations. This work has been

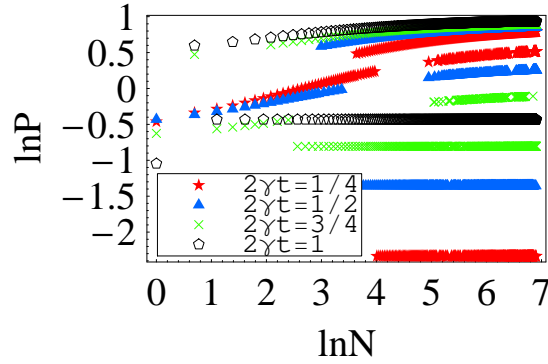


FIG. 15: Ln-ln plots of the improvement in the sensitivity P v.s. the number of the qubits N (up to 10^3) with different damping rate γ : $2\gamma t = 0$ (yellow diamonds), $2\gamma t = 0.25$ (red stars), $2\gamma t = 0.5$ (blue triangles), $2\gamma t = 0.75$ (green crosses), $2\gamma t = 1$ (black circles).

supported by the National Natural Science Foundation of China under Grant Nos 11004029 and 11174052, the Natural Science Foundation of Jiangsu Province under Grant No BK2010422, the Ph.D. Program of the Ministry of Education of China, the Excellent Young Teachers Program of Southeast University and the National Basic Research Development Program of China (973 Program) under Grant No 2011CB921203.

-
- [1] C. M. Caves, Phys. Rev. D **23**, 1693 (1981).
 - [2] B. Yurke, Phys. Rev. Lett. **56**, 1515 (1986).
 - [3] M. Kitagawa and M. Ueda, Phys. Rev. Lett. **67**, 1852 (1991).
 - [4] D. Ulam-Orgikh and M. Kitagawa, Phys. Rev. A **64**, 052106 (2001).
 - [5] D. J. Wineland, J. J. Bollinger, W. M. Itano, F. L. Moore and D. J. Heinzen, Phys. Rev. A **46**, R6797 (1992).
 - [6] P. Cappellaro and M. D. Lukin, Phys. Rev. A **80**, 032311 (2009).
 - [7] J. Ma, X. Wang, C. Sun and F. Nori, Phys. Rep. **509**, 89-165 (2011).
 - [8] X. Wang and B. C. Sanders, Phys. Rev. A **68**, 012101 (2003).
 - [9] M. Kitagawa and M. Ueda, Phys. Rev. A **47**, 5138 (1993).
 - [10] J. Jacobson, G. Björt, I. Chuang and Y. Yamamoto, Phys. Rev. Lett. **74**, 4835 (1995).
 - [11] S. F. Huelga, C. Macchiavello, T. Pellizzari, A. K. Ekert, M. B. Plenio and J. I. Cirac, Phys. Rev. Lett. **79**, 3865 (1997).
 - [12] A. André, A. S. Sørensen and M. D. Lukin, Phys. Rev. Lett. **92**, 230801 (2004).
 - [13] L. Pezzé and A. Smerzi, Phys. Rev. Lett. **102**, 100401 (2009).
 - [14] X. Wang, A. Miranowicz, Y. Liu, C. Sun and F. Nori, Phys. Rev. A **81**, 022106 (2010).
 - [15] Z. Sun, Phys. Rev. A **84**, 052307 (2011).
 - [16] H. J. Biregel and R. Raussendorf, Phys. Rev. Lett. **86**, 910 (2001).
 - [17] M. Hein, W. Dür and H. J. Briegel, Phys. Rev. A **69**, 062311 (2004).
 - [18] M. Rosenkranz and D. Jaksch, Phys. Rev. A **79**, 022103 (2009).
 - [19] W. Dür, L. Hartmann, M. Hein, M. Lewenstein and H. J. Briegel, Phys. Rev. Lett. **94**, 097203 (2005).
 - [20] L. Hartmann, J. Calsamiglia, W. Dür and H. J. Briegel, J. Phys. B **40**, S1 (2007).
 - [21] S. Anders, M. B. Plenio, W. Dür, F. Verstraete and H. J. Briegel, Phys. Rev. Lett. **97**, 107206 (2006).
 - [22] G. S. Agarwal and R. P. Puri, Phys. Rev. A **49**, 4968 (1994).
 - [23] N. F. Ramsey, Molecular Beams (Oxford, London 1963).
 - [24] A. André and M. D. Lukin, Phys. Rev. A **65**, 053819 (2002).
 - [25] J. K. Stockton, J. M. Geremia, A. C. Doherty and H. Mabuchi, Phys. Rev. A **67**, 022112 (2003).
 - [26] C. Gross, T. Zibold, E. Nicklas, J. Estève and M. K. Oberthaler, Nature **464**, 1165 (2010).
 - [27] V. Giovannetti, S. Lloyd and L. Maccone, Science **306**, 1330 (2004).